

EXTRACTION OF INFORMATION FROM NOISY 3-YEAR-OLD ATD RESPONSE SIGNALS IN STATIC OUT-OF-POSITION AIRBAG TESTS

**Lan Xu, Guy Nusholtz, Guglielmo Rabbio,
and Gregory Kostyniuk**

DaimlerChrysler Corporation
United States
Paper No. Abs-468

ABSTRACT

This paper presents an approach to analyze experimental data contaminated with noise from Anthropomorphic Test Devices (ATDs). This approach is based on information extraction procedures and they are illustrated through an analysis of Hybrid III 3-year-old and Q3 ATDs test data.

The methodology used for extracting information and ATD test data analysis includes optimized filtering, spectral coherence, auto- and cross-correlation analysis, and Kalman filtering. This work investigates promising techniques of extracting information from noisy ATD signals that are not commonly used in the automotive industry.

INTRODUCTION

Responses from an ATD are available as acceleration, force, moment, and displacement time histories from transducers in the ATD. Typically, the responses from repeated tests are not identical. The causes of the variability are due to many factors. For example, in the airbag out of position tests (OOP), these factors include the inability to exactly reproduce deployment and unfolding of airbags, variations in positioning of an ATD, vehicle environment, sensitivity of an ATD to the test conditions and electronic noise.

Thus, the response of a single test is contaminated with unwanted variability that obscures, to some degree, the underlying response of the ATD. As an example, the test data reported in [1], used to compare the Hybrid III 3-year-old and Q3 ATDs, contained significant unexplained high frequency signal during the air bag out-of-position tests. Such data cannot always be fully analyzed. However, in some instance, it is possible to extract additional information from noisy signals by proper processing.

In this paper, signal processing techniques that might help extract the underlying signal from a noisy response are proposed. An optimized filter determining procedure is outlined. This procedure is used in conjunction with a spectral coherence analysis. These techniques are illustrated by analyzing the ATD response time histories reported in [1]. Based on processed time-histories, comparisons of peak responses, and the repeatability of the 3-year-old ATDs are presented.

METHODOLOGY

Signal Estimation Methods

Signal estimation refers to a process that identifies the informative portion of a signal by eliminating noise from the raw signal. Several methods ([2,3,4]) have been proposed for this task and are briefly discussed in the following.

Filtering and Optimal Butterworth Filter

Filtering is one of the most commonly used signal processing methods. In general, it is assumed that the low frequency aspects of the ATD response time history contain the underlying signals and the high frequency components are primarily noise. It is expected that the high frequency aspects are removed by filtering for ATD response signals. The result is the elimination of the undesired noisy portion of the signals. Figure 1 shows a signal and the filtered result by a 4-th order 300 Hz Butterworth filter.

Since the exact frequency bands that contain the noise are not known, an inappropriate filtering procedure may adversely affect signal estimation. Therefore, a data based procedure that aims to establish proper filtering by identifying frequency bands containing noise is to be sought. In the following, a simple procedure is proposed.

Given repeated raw test data, if no extra information is available on the underlying phenomena, such as controllable sources of noise, physical modeling of the event or knowledge about the relevant spectral bands, then a statistically "best" procedure to obtain the average behavior of the system is to consider the point-wise sample mean of the time histories. An underlying assumption of this choice is that test signals are the sum of an underlying response or mean and a random phenomenon. More specifically, let the N time histories $\{a_i\}_{i=1,\dots,N}$ be given from test data at uniformly spaced sampling times (t_1, \dots, t_M) . The sample mean

$$m(t_k) = \frac{1}{N} \sum_{i=1}^N a_i(t_k) \quad (k=1, \dots, M)$$

is taken as the best estimate of the true mean of the response.

The procedure used to find an "optimal" filtering is based on the minimization of the squared difference of the filtered time histories and the mean m . If F_f is an operator that filters with a single cut-off frequency f , then the following noise to signal average as a function of f is considered,

$$d(f) = \frac{1}{N} \sum_{i=1}^N \|F_f(a_i) - m\| / \|m\| \quad (1)$$

where $\|x\|^2 = \Delta t \sum_{i=1}^M x_i^2$ and $\Delta t = t_2 - t_1$. The optimal cut-off frequency might be searched among those values that makes $d(f)$ as small as possible.

In this paper, F_f is chosen to be a 4-th order Butterworth filter with cut-off frequency f . By choosing f^* , the frequency that minimizes d , F_{f^*} is referred to as the "optimal Butterworth filter".

Wavelet Denoising

Another approach to signal estimation is based on the use of wavelet transforms. A wavelet transform is similar to a Fourier transform. The Fourier transform decomposes signals into sine and cosine functions defined on the whole real axis. A wavelet transform, instead, decomposes signals into wave functions which grow and decay in a small time period. Because of this localization, wavelets efficiently retain local detailed information of a signal and Wavelet-based denoising techniques are very adaptive to signals with uncorrelated noise [3]. Wavelet analysis is being successfully applied in the

areas of signal processing and data compression [3,5] and is a relatively new tool for analyzing ATD time histories. Figure 2 shows the signal and its denoised version by using a wavelet denoising approach. Compared to filtering in Figure 1, wavelet denoising is nonlinear and phase shift variant and has the advantage of greater preservation of the peaks. For example, it preserves 95% of the peak in Figure 2, compared to 62% in Figure 1, and it smoothes the signals between 30~50 milliseconds as shown in Figure 2. A complete discussion of wavelet denoising is beyond the scope of this paper.

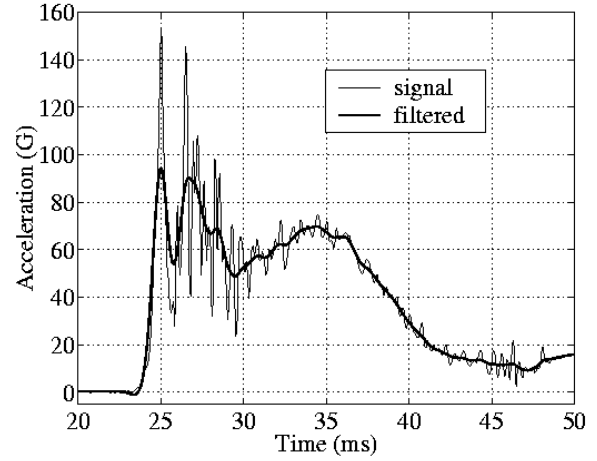


Figure 1 - Signal Filtered by a 4-th order 300 Hz Butterworth Filter.

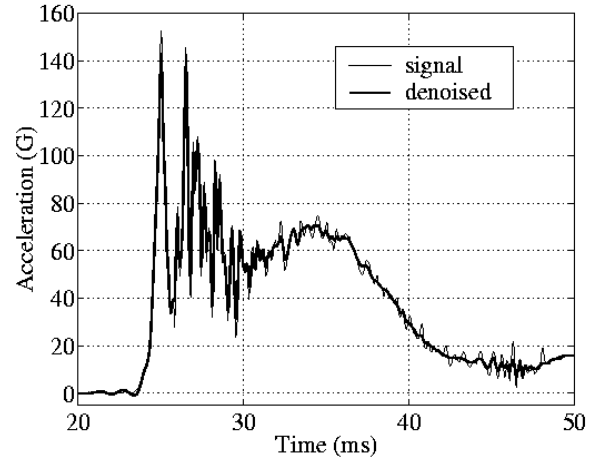


Figure 2 - Signal Denoised by Wavelet.

Spectral Coherence

Spectral coherence [6] is the correlation of signal spectra. The coherence function for two given signals, x and y , is defined as

$$C_{xy}^2(f) = \frac{|P_{xy}(f)|^2}{P_{xx}(f)P_{yy}(f)}$$

where P_{xx} , P_{yy} , and P_{xy} are the power spectrum density functions. Coherence coefficients have values between 0 and 1. A value of 1 indicates identical frequency characteristic of the signals. A value of 0.95 and above is viewed as a very good coherence between the two compared signals. Usually, a value below 0.8 is viewed as that the two signals are incoherent.

ATD Analysis Methods

Correlation Technique

Correlation analysis is used to study the repeatability of ATD responses in this paper. This approach aims at comparing the similarity of the entire time histories of given transducer responses. It uses magnitude and shape to measure the similarity over the whole time-histories. The fundamentals of correlation analysis can be found in [7,8].

An illustration of the terms follows. Figure 3a illustrates two signals with different magnitudes, yet the same shapes and phases. In this case, the coefficient of shape correlation is 1. Figure 3b illustrates two signals with different shapes, yet the same magnitude and phase for which the value of the coefficient of magnitude is 1.

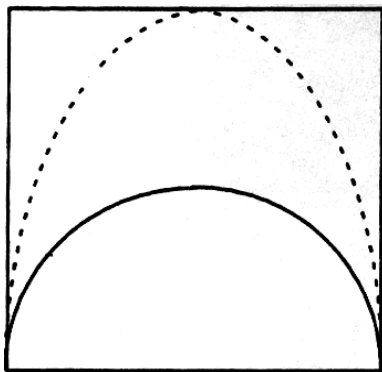


Figure 3a - Signals with Different Magnitude.

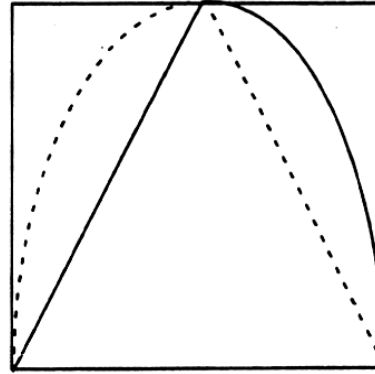


Figure 3b - Signals with Different Shape.

Kalman Filter

A Kalman filter technique is used to calculate ATD sternum velocities. This technique can provide better estimation of ATD chest motion than can be achieved with conventional numerical differentiation or integration of sensor channels [9,10]. This is due to the coupling of related observations through a state model. This approach uses both displacement data of the thorax and acceleration data of the rib and spine. The use of information available in both the accelerometer and displacement signals gives better estimates than those derived from either signal separately.

APPLICATION OF INFORMATION EXTRACTION PROCEDURE TO 3-YEAR-OLD ATD COMPARISON

The Hybrid III 3-year-old and Q3 ATDs are designed to be representative of a 3-year-old human. As indicated in [1,11,12], the Hybrid III 3-year-old ATD was designed primarily for frontal impacts and the Q3 ATD was for both frontal and lateral impacts. The major differences between the two ATDs were discussed in [1].

The two ATDs have been evaluated by using OOP tests ([1]). Two different seat-mounted side airbag systems (SAB), one door-mounted SAB system and one frontal passenger airbag system (PAB) were used with airbag OOP tests. Five different positions (position 1 through 5) were tested with the seat-mounted SAB. Two positions were tested with the door-mounted SAB (position 6 and 7), and one position (position 8) was tested with the frontal PAB. Each test was conducted three times. Detailed information on ATD positions is described in [1]. In most positions, the ATDs were primarily frontally loaded. Only in three test conditions, the ATDs were

primarily laterally loaded. These tests are, position 3 with seat SAB 1 and seat SAB 2, as well as position 7 with door SAB.

The Hybrid III 3-year-old ATD, in this section will be referred to as H3. Measurements of the H3 and the Q3 ATDs are compared in terms of percentage differences relative to the smaller one whenever a general trend is observed in the test results.

Signal Processing

Optimal Butterworth filtering and wavelet denoising were used to investigate the best way to process the H3 and Q3 ATDs' response time-histories. It is found that the use of an optimal filter is appropriate for the ATD impact response, when the whole time-histories are of interest. If the peaks are also to be identified, wavelet denoising would be appropriate. Analysis of the average spectral coherence of signals to their mean is used to validate the optimal frequency procedure.

Three types of noise to signal average curve characteristics have been observed. Figure 4a shows typical noise to signal average curves. The raw signals for Figure 4a are shown in Figure 4b. It indicates that if the cut-off frequency used is less than 200 Hz, some information might be lost. Cut-off frequencies 200 Hz and above are acceptable to estimate the true signal. This noise to signal average characteristic has been observed in many cases studied. They are typically seen in head/chest/sternum accelerations, and most neck forces/moments and chest deflections. Figure 4c shows the spectral coherence of the signals. It indicates that the signals are coherent until the cut-off frequency reaches 500Hz.

Figure 5a shows another type of noise to signal average curves. The raw signals for the Figure 5a are shown in Figure 5b. The results indicate that the optimal cut-off frequency is around 300 Hz. In practice, low values of noise to signal average are obtained using the cut-off frequencies between 250 to 500 Hz. This type of noise to signal average characteristic is observed in some cases studied. They are typically seen in rib accelerations. Figure 5c shows the spectral coherence of the signals. It indicates that the signals and their mean are correlated acceptably within the frequency range 0 to 1000 Hz.

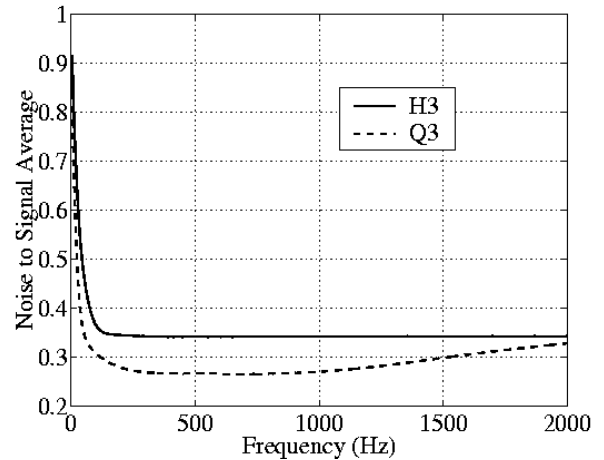


Figure 4a - Noise to Signal Average for the Responses in Figure 4b.

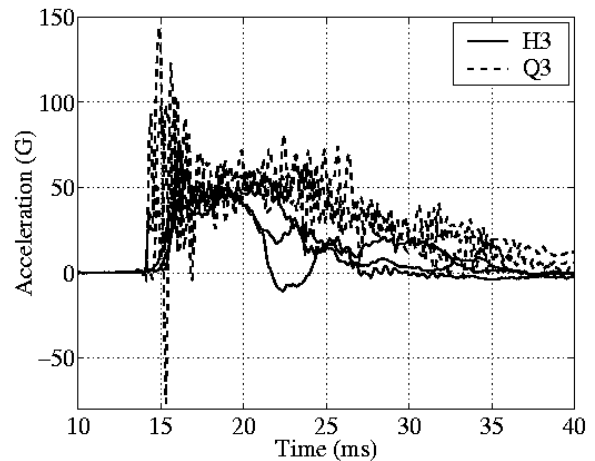


Figure 4b - Head Resultant Acceleration in Position 2 With Seat SAB 2.

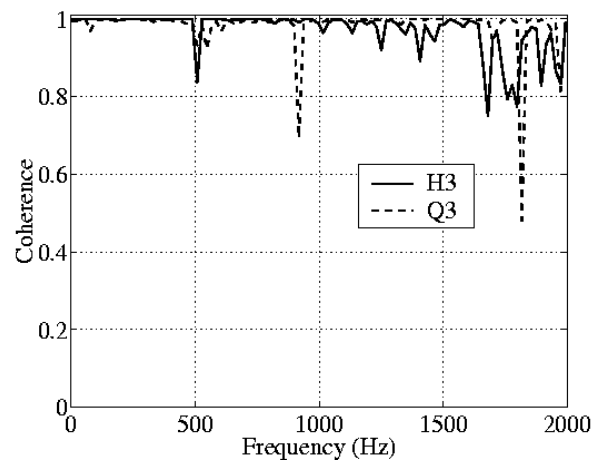


Figure 4c - Spectral Coherence for the Responses in Figure 4b.

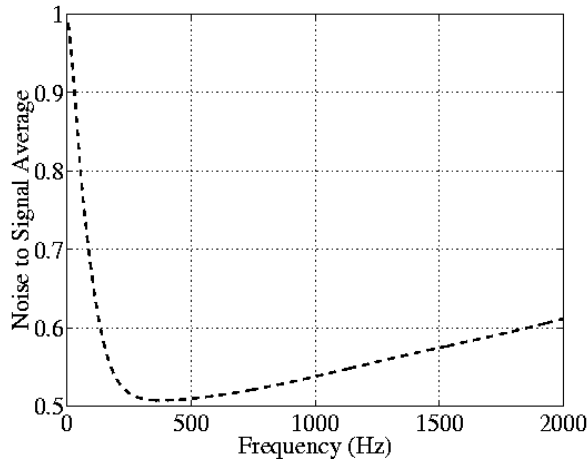


Figure 5a - Noise to Signal Average for the Responses in Figure 5b.

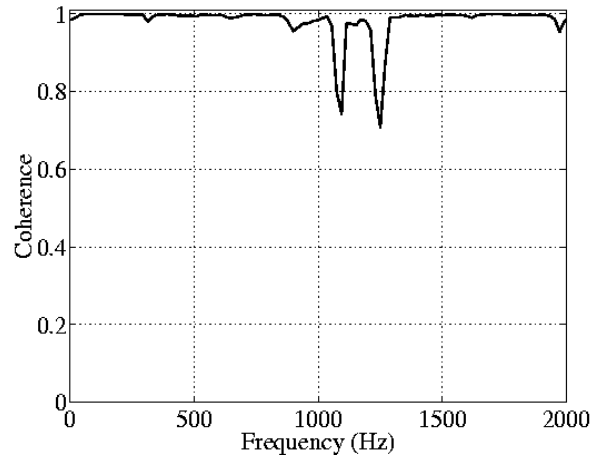


Figure 5c - Spectral Coherence for the Responses in Figure 5b.

Figure 6a shows the characteristic of an interesting noise to signal average curve. The raw signals used for Figure 6a are shown in Figure 6b. It indicates that the use of a Butterworth filter is inappropriate to estimate the given signals. In such cases, filtering can not improve noise to signal ratio because the optimal filter frequency is too low. This is due to large inconsistencies of low frequency components of the signals, caused by a large variability along the entire time histories between repeated tests. This type of noise to signal average characteristic represents a few of the cases studied. Figure 6c shows the spectral coherence of the signals. These signals are not coherent. In other words, the responses are not repeatable.

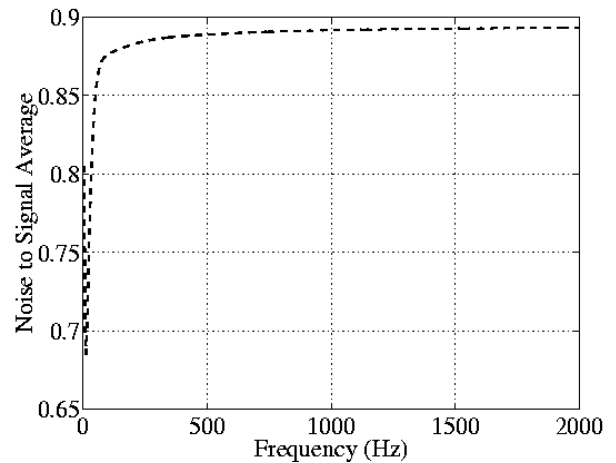


Figure 6a- Noise to Signal Average for the Responses in Figure 6b.

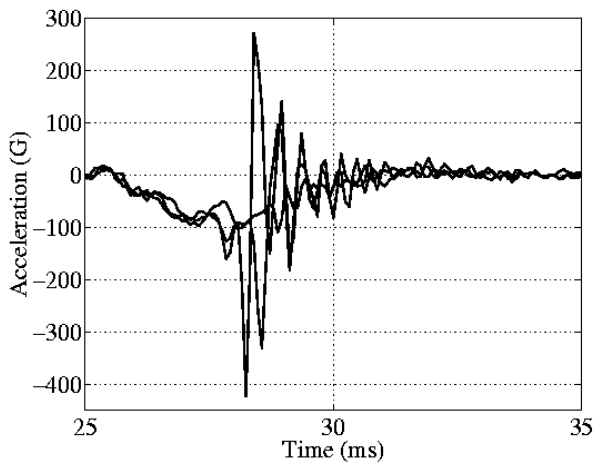


Figure 5b - H3 Chest Resultant Acceleration in Seat SAB 2, Position 2.

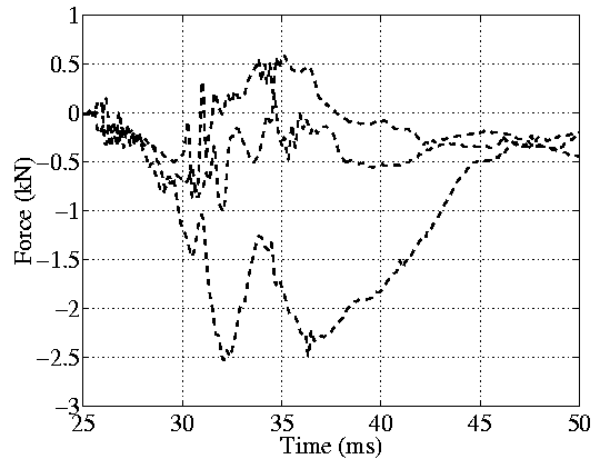


Figure 6b - Q3 Upper Neck Shear Force in Position 5 with Seat SAB 2.

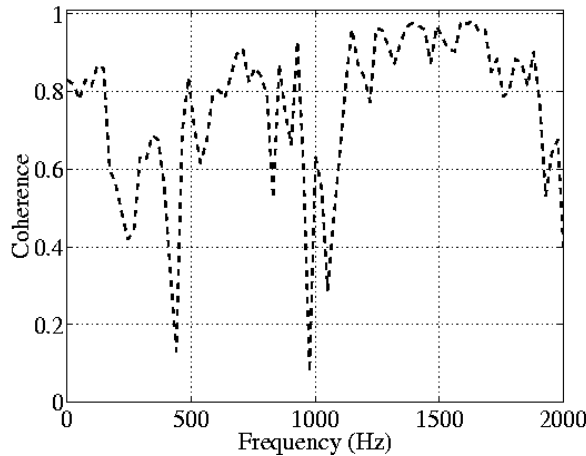


Figure 6c - Spectral Coherence for the Responses in Figure 6b.

All the response time histories in the direction for which signal is the highest are processed by an optimal Butterworth filter. A review of the optimized filtering determining procedure in conjunction with spectral coherence analysis indicates that the overall best cut-off frequency for the Butterworth filter is around 300Hz. Even though a 4-th order 300 Hz Butterworth filter is not the best choice for each individual test, overall it is reasonable if a single filter is to be used for all data. Therefore, the analysis below is based on the data processed by a 4-th order

300 Hz Butterworth filter. The data polarities presented in this paper are in accordance with SAE J211.

ATD Peak Response Comparison

Table 6 presents the peak value comparison between the H3 ATD and Q3 ATD. The values in the table are the average of the peaks from three repeated tests. The observations are made as follows.

Head Resultant Acceleration

- With seat SAB system 1, H3>=Q3 in four cases out of five.
- With seat SAB system 2, Q3>H3 in all five cases. Q3 is 50% greater on average.
- With door SAB system, H3>Q3 in one case, and Q3>H3 in the other case.
- With PAB system, Q3>H3. Q3 is 45% greater.

Upper Neck Force in Posterior to Anterior (PA) Direction (X)

- With seat SAB system 1, H3>Q3 in four cases out of five.

Table 6. Peak Response Comparison

	Head Resultant Acc.(g)		Neck X-Force(N)		Neck Z-Force(N)		Neck Y-Moment(Nm)	
	H3	Q3	H3	Q3	H3	Q3	H3	Q3
Seat SAB. 1, Pos. 1	63.0	77.5	-362.6	-275.1	776.4	603.0	-***	-
Seat SAB. 1; Pos. 2	44.1	23.0	340.1	69.0	576.1	434.3	-	-
Seat SAB. 1, Pos. 3	57.4	58.3	474.4	176.1	437.0	851.9	-	-
Seat SAB. 1; Pos. 4	58.1	34.4	238.0	262.8	685.4	356.8	-	-
Seat SAB. 1, Pos. 5	51.4	42.1	-200.8	-148.8	1167.5	630.7	-	-
Seat SAB. 2; Pos. 1	100.0	111.4	210.7	513.1	819.7	1079.3	-15.7	-4.5
Seat SAB. 2; Pos. 2	39.3	73.1	270.8	297.7	930.6	1431.4	-12.0	-8.7
Seat SAB. 2; Pos. 3	28.6	92.6	-406.6	-209.5	663.4	764.5	-24.5	-11.8
Seat SAB. 2; Pos. 4	58.9	79.8	735.5	861.9	648.1	749.5	26.4	27.0
Seat SAB. 2; Pos. 5	36.6	58.6	380.8	-	817.6	1299.6	-15.4	-9.1
Door SAB; Pos. 6	20.8	37.5	-377.8	-	828.8	922.8	-18.3	-13.1
Door SAB; Pos. 7	74.9	66.0	-141.2	-81.9	700.2	401.5	-4.5	-3.8
PAB; Pso. 8	154.8	201.1	971.7	1160.2	2033.8	2940.4	-50.6	-57.9

*: Seat SAB 1, Pos. 1 represent that tests is with seat-mounted SAB system 1 and the ATD is in position 1.

** : The chest deflections are in the Y-direction. All others are the deflection in X direction.

***: -sign in the table represents that the result is not available either due to collecting data or filtering failure

Table 6. Peak Response comparison (Continued)

	Chest Resultant Acc.(g)		Rib Y-Acc.(g)		Chest Deflection(mm)		Sternum Velocity(m/s)	
	H3	Q3	H3	Q3	H3	Q3	H3	Q3
Seat SAB. 1; Pos. 1	27.6	40.1	-7.4	-6.4	-1.7	-3.2	-0.4	-0.56
Seat SAB. 1; Pos. 2	34.4	26.4	47.5	31.53	-26.7	-7.0	-6.4	-1.8

Seat SAB. 1, Pos. 3	43.2	49.1	-19.8	-94.9	-29.8	-2.5**	-6.6	-2.1**
Seat SAB. 1; Pos. 4	31.8	56.1	-16.8	-7.3	-2.8	-2.6	-0.6	-1.0
Seat SAB. 1, Pos. 5	34.1	45.6	59.1	25.4	-18.1	-9.0	-5.0	-2.3
Seat SAB. 2; Pos. 1	67.8	138.0	-38.5	-33.3	-2.7	-4.5	-0.80	-1.6
Seat SAB. 2; Pos. 2	131.2	124.8	353.7	547.8	-	-31.0	-	-12.6
Seat SAB. 2; Pos. 3	113.4	169.3	-	-574.4	-16.6	-13.4**	-5.5	-10.6**
Seat SAB. 2; Pos. 4	130.4	254.3	-39.0	-76.5	-6.7	-7.3	-1.6	-2.9
Seat SAB. 2; Pos. 5	62.7	110.9	379.8	279.7	-38.9	-34.3	-12.8	-9.4
Door SAB; Pos. 6	34.9	51.0	-	-414.1	-30.3	-17.2	-5.1	-4.3
Door SAB; Pos.7	21.0	29.0	-20.1	-43.9	-1.3	7.9**	-0.2	7.3**
PAB; Pos.8	48.8	104.8	-	-	-11.0	6.3	-2.4	-3.1

- With seat SAB system 2, Q3>H3 in three cases out of four.
- With door SAB system, H3>Q3 in both cases.
- With PAB system, Q3>H3. Q3 is 20% greater.

Upper Neck Force in Superior to Inferior (SI) Direction (Z)

- With seat SAB system 1, H3>Q3 in four cases out of five.
- With seat SAB system 2, Q3>H3 in all five cases. Q3 is about 35% greater on average.
- With door SAB system, H3>Q3 in one case, and Q3>H3 in the other case.
- With PAB system, Q3>H3. Q3 is 45% greater.

Upper Neck Moment in Left to Right (LR) Direction (Y)

- With seat SAB system 2, H3≥Q3 in all five cases, either extension or flexion. H3 is about 45% greater on average.
- With door SEAT SAB system, H3>Q3 in both cases. H3 is about 40% greater.
- With PAB system, Q3>H3. Q3 is 15% greater.

Chest Resultant Acceleration

- With seat SAB system 1, Q3>H3 in four cases out of five.
- With seat SAB system 2, Q3>H3 in four cases out of five. Among them, peak in Q3 is more than 80% greater than that in the H3 in three cases.
- With door SAB system, Q3>H3 in both cases. Q3>H3 is about 45% greater.
- With PAB system, Q3>H3. Q3 is about 120% greater.

Rib Lateral Acceleration (Y)

The accelerations compared in the Table are those in the positive Y direction if the ADT was struck on left side or negative Y if struck on right side.

- With seat SAB system 1, H3>Q3 in four cases out of five.
- With seat SAB system 2, Q3>H3 in two cases out of four.
- With door SAB system, Q3>H3 in all cases. Q3 is 100% greater on average.
- With PAB system, Q3>H3. Q3 is about 110% greater.

Chest PA Deflection

ATD chest deflections produced in position 1 and 4 are insignificant. Two ATD chest deflections from position 3 and position 7 are not comparable because the measurements are in two different directions. These facts are true for sternum velocities.

- With seat SAB system 1, H3>Q3 in all two significant and comparable cases, position 2 and 5. H3 is about 210% greater, or 15 mm greater on average.
- With seat SAB system 2, H3>Q3 in one significant and comparable case, position 5. H3 is 15% greater.
- With door SEAT SAB system, H3>Q3 in one comparable case, position 6. H3 is about 75% greater.

Sternum AP Velocity

- With seat SAB system 1, H3>Q3 in all two significant and comparable cases, position 2 and 5. H3 is 178% greater, or 3.65m/s greater on average.
- With seat SAB system 2, H3>Q3 in one significant and comparable case, position 5. H3 is 36% greater.

- With door SAB system, $H3 > Q3$ in one comparable case, position 6. H3 is 20% greater.
- With PAB system, $Q3 > H3$. Q3 is 30% greater.

In summary, trends of a comparison between the ATD responses, in general, depend on ATD regions and test positions. Nevertheless, extensional moments at the upper neck region in the H3 are consistently higher than those in the Q3 in the tests with SAB systems. The chest resultant accelerations in the Q3 are higher than those in the H3 in almost all the cases while the opposite occurs for chest deflections.

ATD Response Repeatability Comparison

The correlation analysis is used to study the similarity level of signals from repeated tests in terms of both magnitude and shape. The magnitude and shape correlation coefficients are presented in Tables 8 and 9.

Correlation coefficients can have values between 0 and 1. A value of 1 indicates identical characteristic of the two compared signals. A value of 0 indicates orthogonality. The values in the tables are the mean

Table 8. Magnitude Correlation

	Head Reslt. Acc		Neck X-Force		Neck Z-Force		Neck Y-		Chest Reslt. Acc		Rib Y-Acc		Chest X or Y-Def.	
	H3	Q3	H3	Q3	H3	Q3	H3	Q3	H3	Q3	H3	Q3	H3	Q3
Seat SAB. 1; Pos. 1	0.6822	0.6211	0.8338	0.4558	-	-	0.3394	0.8163	0.8810	0.6182	0.7778	0.6936	0.3832	0.8042
Seat SAB. 1; Pos. 2	0.2701	0.4845	0.3910	0.2946	-	-	0.4188	0.5122	0.9361	0.4965	0.7164	0.4504	0.7380	0.3259
Seat SAB. 1, Pos. 3	0.8922	0.9061	0.3736	0.7426	-	-	0.5476	0.8495	0.9492	0.8922	0.7084	0.4799	0.6060	0.6193
Seat SAB. 1; Pos. 4	0.6310	0.7608	0.4512	0.6489	-	-	0.7648	0.6459	0.9510	0.5882	0.7929	0.7114	0.3989	0.8075
Seat SAB. 1, Pos. 5	0.3921	0.5687	0.0561	0.2709	-	-	0.2054	0.7395	0.6932	0.6623	0.4489	0.8070	0.6372	0.8034
Seat SAB. 2; Pos. 1	0.8439	0.9110	0.6994	0.8070	0.5909	0.8547	0.6536	0.7619	0.9239	0.7024	0.9259	0.5588	0.7714	0.7378
Seat SAB. 2; Pos. 2	0.6900	0.9086	0.8960	0.7258	0.7490	0.8614	0.6325	0.9168	0.8411	0.9040	0.7771	0.8713	-	-
Seat SAB. 2; Pos. 3	0.8937	0.4575	0.9561	0.1127	0.9152	0.0727	0.8990	0.5588	0.9936	0.8057	0.8612	0.8933	0.5910	0.7737
Seat SAB. 2; Pos. 4	0.9581	0.6807	0.9745	0.7138	0.8622	0.5114	0.8264	0.3809	0.9554	0.8927	0.8399	0.7540	0.9103	0.8786
Seat SAB. 2; Pos. 5	0.9351	0.8816	0.6868	-	0.8622	0.7932	0.5986	0.9155	0.9696	0.6629	0.8376	0.5016	0.9393	-
Door SAB; Pos. 6	0.6505	0.6289	0.6460	-	0.7040	0.2231	0.6318	0.4814	0.9333	0.6361	0.8800	0.7751	0.8806	0.6126
Door SAB; Pos.7	0.9230	0.9009	0.6054	0.6982	0.3804	0.4833	0.4667	0.8998	0.9123	0.8836	0.9528	0.6791	0.6441	0.8470
PAB; Pos.8	0.8994	0.9470	0.5792	0.8288	0.5155	0.8705	0.8028	0.6825	0.7984	0.7292	0.3654	0.6989	0.5797	0.7170

Table 9. Shape Correlation

	Head Reslt. Acc		Neck X-Force		Neck Z-Force		Neck Y-Moment		Chest Reslt. Acc		Rib Y-Acc		Chest X or Y-Def.	
	H3	Q3	H3	Q3	H3	Q3	H3	Q3	H3	Q3	H3	Q3	H3	Q3
Seat SAB. 1; Pos. 1	0.9248	0.9006	0.9241	0.3281	0.6978	0.7344	-	-	0.9434	0.8979	0.6842	0.7580	0.7189	0.8193
Seat SAB. 1; Pos. 2	0.8571	0.8027	0.7663	0.1521	0.6797	0.8125	-	-	0.8019	0.8695	0.6343	0.6222	0.8265	0.9007
Seat SAB. 1, Pos. 3	0.8765	0.9470	0.4772	0.6178	0.7852	0.9004	-	-	0.9680	0.8765	0.7262	0.6299	0.9418	0.4786
Seat SAB. 1; Pos. 4	0.9520	0.8745	0.4494	0.8336	0.6944	0.8548	-	-	0.8849	0.8566	0.8011	0.8019	0.6861	0.4668
Seat SAB. 1, Pos. 5	0.8819	0.7574	0.2920	0.6626	0.4266	0.8465	-	-	0.6075	0.8348	0.3174	0.3828	0.5889	0.8132
Seat SAB. 2; Pos. 1	0.9392	0.9654	0.7574	0.9176	0.9344	0.9688	0.9078	0.7015	0.9708	0.9549	0.8018	0.7739	0.9421	0.9446
Seat SAB. 2; Pos. 2	0.9621	0.9571	0.9541	0.6806	0.8388	0.9614	0.9507	0.7744	0.9209	0.9581	0.9688	0.9782	-	-
Seat SAB. 2; Pos. 3	0.9640	0.7583	0.9794	0.4091	0.9430	0.5696	0.9773	0.3815	0.9862	0.8388	0.7840	0.8925	0.9676	0.8890
Seat SAB. 2; Pos. 4	0.9887	0.9464	0.9830	0.7922	0.9014	0.8191	0.9606	0.6242	0.9910	0.9557	0.7241	0.7862	0.9737	0.7713
Seat SAB. 2; Pos. 5	0.9785	0.9760	0.9348	-	0.9097	0.9451	0.9606	0.3076	0.9071	0.9043	0.9838	0.8834	0.9840	-
Door SAB; Pos.6	0.9649	0.9461	0.9700	-	0.9776	0.9263	0.9833	0.7779	0.9846	0.8456	0.9052	0.8548	0.9959	0.8484
Door SAB; Pos.7	0.9742	0.9602	0.8073	0.0003	0.6163	0.8267	0.2542	0.0402	0.9544	0.9531	0.9135	0.1928	0.7359	0.9841
PAB; Pos.8	0.9460	0.8506	0.4854	0.9267	0.9472	0.9583	0.5470	0.9171	0.9383	0.8899	0.3270	0.1794	0.8975	0.5556

Table 10. Comparison of ATD Response Repeatability

	Number of Cases for Magnitude Where		Number of Cases for Shape Where	
	H3 > Q3	Q3 > H3	H3 > Q3	Q3 > H3
Head Resultant Acceleration	6	7	11	2
Upper Neck X-Force	7	6	8	5
Upper Neck Z-Force	4	9	3	10
Upper Neck Y-Moment	4	4	7	1
Chest Resultant Acceleration	12	1	10	5
Rib Y-Acceleration	9	4	8	5
Chest Deflection	5	7	7	5

of the correlation coefficients for three signals from the repeated tests.

For the purpose of quantitatively understanding the values of the correlation, the following example should be useful. For the chest or pelvis acceleration response in typical FMVSS 208 sled tests, a value higher than .95 indicates an identical within test to test variation. A value between .8 and .95 indicates similar response, but not within test to test variation. A value lower than .8 indicates dissimilar responses.

The Correlation Coefficients (CC) of the ATD response at different body regions are presented in Tables 8 and 9. Based on the Tables, some observations about magnitude and shape correlation can be made as follows:

Magnitude Correlation

- For H3, CC >0.95 in 8% of all cases;
0.8 < CC < 0.95 in 33% of all cases
CC < 0.8 in 59% of all cases
- For Q3, CC >0.95 in 0% of all cases;
0.8 < CC < 0.95 in 35% of all cases
CC < 0.8 in 65% of all cases

Shape Correlation

- For H3, CC >0.95 in 34% of all cases;
0.8 < CC < 0.95 in 35% of all cases
CC < 0.8 in 31% of all cases
- For Q3, CC >0.95 in 16% of all cases;
0.8 < CC < 0.95 in 41% of all cases
CC < 0.8 in 43% of all cases

As to the magnitude correlation, the results indicate that for more than half of the cases, the repeatability level for both ATDs is poor (CC < 0.8). As to the shape correlation, more than 30% of the cases for the

H3, and more than 4 0% of the cases for the Q3 show poor repeatability.

Table 10 is derived from Tables 8 and 9. It shows the repeatability comparison between the two ATDs. It is concluded from columns 4 and 5 in Table 10 that the H3 shows better shape correlation in all the cases except for one case of upper neck Z-force. In terms of magnitude, the Q3 shows better correlation than the H3 in 3 cases out of 7 and the H3 shows better correlation than the Q3 in 3 cases out of 7; and in the other case they are equal. The H3 ATD shows better overall level of repeatability in chest, and rib accelerations. The Q3 shows better overall level of repeatability in the upper neck Z-force.

DISCUSSION

The observations presented in this paper are based on specially processed raw ATD response time-histories. When comparing ATD responses, the procedures in SAE J211 are generally used to process the raw signals. However, application of a predetermined signal processing methods, such as SAE J211, may not allow an optimal extraction of information. Alternative signal processing methods could be applied to further analyze the test data. An optimal filtering procedure in conjunction with spectral coherence analysis can be used to determine cut-off frequencies when repeated test data are available. Consequently, signal to noise ratio is improved in the response time-histories, which may make the peak response comparison and repeatability study by correlation analysis more reliable.

In general, the results of the comparison between any two ATDs are affected by test conditions, test types, instrumentations, test facilities, as well as the differences in the ATDs. As a result, the potential of unexplained noise increases and the experimental comparison may not represent the true differences between two ATDs. To minimize the effects of

noise, it is advantageous to try to extract as much information as possible. Higher amount of information may be extracted through the use of signal processing procedures, such as those outlined in this paper. Optimization of signal to noise ratio of given transducer time-histories can be accomplished through the use of a data based process when repeated tests are available. The correlation analysis for the repeatability comparison uses more information, such as the whole time histories, than just using the peak information to analyze a ATD response. The Kalman filter for the sternum velocity calculation uses more information, both accelerations and displacements on ATD chest, compared to traditional methods.

A comparison between the Q3 and Hybrid III 3-year-old ATD in this paper is performed to illustrate the use of the signal processing procedure discussed above to enhance ATD analysis. The results indicate that the peak responses of chest resultant acceleration in the Q3 are higher in general, compared to that in the Hybrid III 3-year-old ATD. However, the chest deflections in the Q3 are lower than the Hybrid III 3-year-old. The peak extensional moment responses at the upper neck location of the Q3 are lower than that with the Hybrid III 3-year-old ATD in the tests with SAB systems. The Hybrid III 3-year-old ATD generally produces more repeatable responses than the Q3 in the airbag out-of-position tests.

CONCLUSION

This is a limited presentation of methods to extract information from noisy signals. Several procedures have been presented, including optimal filtering, wavelet denoising, spectral coherence, correlation analysis, and Kalman filtering. Although some heuristic judgements have been utilized, they offer reasonable procedures to extract information from noisy impact test signals such as ATD responses. These procedures can be used to analyze ATD responses and potentially extract more information than conventional analysis procedures.

ACKNOWLEDGMENTS

The authors appreciate the contributions from Dr. Paul Eagle of DaimlerChrysler.

REFERENCES

1. Jeffery Berliner, etc., "Comparative Evaluation of the Q3 and Hybrid III 3-Year-Old Dummies in

Biofidelity and Static Out-of-Position Airbag Tests", STAPP Conference, 2000

2. R.W. Hamming, "Digital Filters", Prentice-Hall, 1989

3. Donald B. Percival and Andrew T. Walden, "Wavelet Method for Time Series Analysis", Cambridge University Press, 2000

4. Guy, S. Nusholtz, "A Simple Non-Linear Shift-Variant Process/Filter for Reducing Gaussian Noise in Impact Signals", J. of Sound and Vibration, 1988 120(3), 567-585

5. Ingrid Daubechies, "Ten Lectures on Wavelets", CBMS-NSF, Regional Conference Series in applied Mathematics, 1992

6. David J. DeFatta, etc. "Digital Signal Processing: A system Design Approach," John Wiley & Sons, Inc., 1988

7. G. S. Nusholtz, L. Xu, V. Agaram, J. Athey, J. Balsler, R. P. Daniel, R. W. Hultman, S. Kirkish, H. Mertz, D. Parks, J. Prater, S. Rouhana, and R. Scherer, "Comparison of the Pre-Prototype NHTSA Advanced DUMMY to the Hybrid III," SAE 971141, 1997.

8. L. Xu, V. Agaram, S. Rouhana, R. Hultman, G. W. Kostyniuk, J. McCleary, H. Mertz, G. S. Nusholtz, and R. Scherer, "Repeatability Evaluation of the Pre-Prototype NHTSA Advanced Dummy Compared to the Hybrid III," SAE 2000-01-0165, 2000

9. Guy S Nusholtz and Paul J Eagle, "Kalman Filter Estimation of Chest Velocity", International Journal of Crash 2000, Vol 5, No. 4.

10. G. S. Nusholtz, P. J. Eagle, and L. C. Cattani, "Use of a Kalman Filter to Improve the Estimation of Dummy Response During Impact", SAE Paper 1999-01-0707, 1999.

11. A. Irwin, and H. J. Mertz, "Biomechanical Basis for CRABI and Hybrid III Child Dummies," SAE 973317, 1997.

12. M. R. van Ratingen, D. Twisk, M. Schrooten, M. C. Beusenberg, A. Barns, and G. Platten, "Biomechanically Based Design and Performance Targets for a 3-Year Old Child Crash Dummy for Frontal and Side Impact," SAE 973316, 1997

